International Journal of Robotics and Control Systems
Vol. 5, No. 1, 2025, pp. 47-67
ISSN 2775-2658
http://pubs2.ascee.org/index.php/ijrcs

Theoretical and Experimental Investigation of the Effect of Linear Fluid Power Control System Design on its Static and Dynamic Performance

A. I. Qassim [a,1,*], Tahany W. Sadak [b,2,*], Mahassen Rizk [a,3]

[a] Faculty of Engineering, Production Eng. Mechanical Design Department, Minia University, Minia, 61511, Egypt
[b] Faculty of Engineering, Mechanical Department, Beni-Suef University, Beni-Suef, 62511, Beni-Suef, Egypt
[1] A.iqassim@yahoo.com; [2] Tahany@eng.bsu.edu.eg; [3] mahassenri@yahoo.com
* Corresponding Author

ARTICLE INFO

Article history
Received August 03, 2024
Revised November 30, 2024
Accepted December 02, 2024

Keywords
Fluids Power Control Systems;
Servo Control Valve;
Proportional Flow Control Valve;
Hydraulic Control Valve

ABSTRACT

Fluid power control systems are widely used in automated systems like manufacturing, biomedical treatments, and food handling, as well as in optimizing aircraft wing design, mobile applications, and thermal management in electronic devices, energy transformation, and aerospace applications. This study investigated the static and dynamic characteristics of a linear fluid power control system utilizing either a servo control valve (SV) or a proportional directional flow control valve (PV). The study focused on evaluating performance differences between these two valve types while maintaining a constant oil temperature at 30°C. Experimental tests were conducted under varying supply pressures, loads, and valve types. A system was built to conduct real-time experiments. In this paper we studied the effect of valve flow rate at full opening, the actual supply pressure-decay, and studied the effect of the loading system on the performance. The aim of this paper is to find out which control valve is better in static and dynamic performance in real-world. Through comparing two hydraulic control valves designs, the experiment results show that the servo control valve (SV) offers a clear advantage over the proportional directional flow control valve (PV) in linear fluid power control systems operating at a constant temperature. The SV designs demonstrated superior performance in terms of flow rate, pressure retention, and dynamic response. This makes SV an optimal choice for applications requiring high flow rates, consistent pressure, and precise, rapid adjustments, especially in high-speed operations.

This is an open-access article under the CC–BY-SA license.

1. Introduction

Fluids have been used for the benefit of humans, such water supply, agricultural promotion, and resilience, in urban areas since antiquity, long before humans developed a deep understanding of science and how to harness it [1]-[3]. Fluid power is the technology that involves the production, control, and transmission of forces to move mechanical elements or systems using pressurized fluids in a safe environment [4]-[7]. Fluid power hydraulic circuits are critical components in various industrial applications, enabling precise movement and force. These include basic circuits, directional control circuits, flow control circuits, and combination circuits. Several real-world

applications use combinations of these fundamental circuits to perform specialized tasks [7], [8]. In hydraulic circuits, a reservoir stores hydraulic fluid. The hydraulic pump supplies fluid throughout the system and converts the mechanical energy into hydraulic energy. Valves regulate fluid flow and, when necessary, release excess pressure from the system. The hydraulic actuator converts the stored energy into mechanical energy [7].

Fluid power systems offer a superior power-to-weight ratio and high power density compared to electric systems, along with precise control, making them valuable in modern industries, especially mobile machines [9]-[13]. Fluid power control systems are widely used in automated systems like manufacturing, biomedical treatments, and food handling, as well as in optimizing aircraft wing design, mobile applications, and thermal management in electronic devices, energy transformation, and aerospace applications [14]-[18]. Despite its precision, hydraulic control system faces more challenges than electronic systems. Acquiring precise control over position, speed, or pressure necessitates sophisticated valve arrangements and modern controllers. Energy-saving solutions to hydraulic control systems have made substantial progress because of the increasing demand for efficiency in various industrial applications. Recent studies have highlighted advancements in control strategies, system designs, and hybrid technologies that collectively contribute to energy conservation [19]-[23]. Traditional hydraulic systems predominantly employ analog spool valves, including proportional and servo valves, functioning as directional control valves in a range of industrial and aerospace applications necessitating elevated precision and rapid response [24]-[28]. The proportional and servo valve mechanisms are continuously regulated by an analog voltage. These systems offer superior control accuracy and excellent dynamic response [29], [30].

Electrohydraulic servo valves are divided into two types: single-stage and two-stage. In the single-stage design, the sliding spool is directly controlled by integrated electronics via a linear force motor. In the two-stage design, the sliding spool is positioned in the main stage and is controlled indirectly by electronics using a pilot stage. The last of these can be outfitted with either a centralized spring for mechanical feedback or a linear variable differential transformer (LVDT) sensor for electrical feedback [31], [32]. Servo valves offer fast dynamic performance, precise control, compact size, excellent load matching, high environmental stiffness, a wide range of adjustable speeds, and increased reliability while maintaining rapid response times and high flow rates [33]. On the contrary, proportional valves are often a single-stage system in which the sliding spool is centered by springs within the valve body and immediately activated by two proportionate solenoids located on either side of the valve [34], [35]. There are detailed analyses available to investigate the fluid dynamic behavior of commercial hydraulic proportional valves. These calculations allow us to understand how flow forces and cavitation events affect the efficiency of this type of spool valve [36].

The recently developed proportional directional valve, equipped with an independently regulated pilot stage, significantly enhances dynamic properties and control precision by reducing dead space and damping influences, while simultaneously improving response velocity and tracking fidelity [37]-[41]. The proportional flow control valve was designed to mitigate leakage, thereby achieving an energy efficiency improvement [42]. Many research projects have examined the static and dynamic behaviors of hydraulic valves, which are crucial to their performance in various applications. Static characteristics like static pressure control relate to the valve's behavior under steady-state conditions. Dynamic characteristics, on the other hand, involve the valve's ability to adapt to changing conditions to improve response time and bandwidth [43]-[48]. On the other side, the viscosity of a fluid decreases as its temperature increases. In liquids, cohesive forces between molecules dominate molecular momentum transfer due to the close proximity of the molecules [10]. Conversely, the viscosity of fluids increases as their pressure increases. Therefore, when designing hydraulic systems that operate over a wide range of pressures, it is essential to consider the effects of viscosity variation. Numerous articles investigate the impact of various factors, such as temperature, pressure, and flow rate, on hydraulic system performance [49]-[54]. This research presents a comparative investigation of the static and dynamic characteristics of fluid power control systems when using either a servo control valve or a proportional directional flow control valve in

connection with system design. The study explores the various factors that influence the system's ability to achieve linear, position-controlled movement.

In summary, this paper navigates the theoretical and experimental investigation of the effect of linear fluid power control system design on its static and dynamic performance. This study focuses on the hydraulic circuit's control stage, examining the performance and characteristics of two different designs of hydraulic control valves to determine which is most effective for regulating hydraulic actuators. The most suitable system design can be selected based on cost, optimal performance, and energy consumption. The findings give useful information for selecting the right valve for a variety of industrial applications in the real world. The contributions that the study introduces are listed below:

- The paper investigates the dynamic and static behavior of the servo control valves and proportional directional control valves when considering the constant temperature.
- The performance comparison analysis identified the strengths and weaknesses of each hydraulic control valve.
- The study showed that the servo control valve has a higher response time compared to the proportional control valve.
- The study may be expanded to include different types of hydraulic control valves.

The research study is described as follows: Section 2 outlines the system design and components of the fluid power control system, which is connected to two hydraulic control valves. Section 3 describes experimental methodologies for measuring variations in the system supply pressure and pressure response in the two chambers of the hydraulic actuator during piston movement and displacement. Section 4 evaluates the static and dynamic flow rate performances, supply pressure degradation, and stroke period throughout the system operation. The experimental results are compared. The comparison is between attaching a proportional directional flow control valve and connecting it to a servo flow control valve. Finally, Section 5 presents the conclusions.

2. System Design and Calibration

The system was designed to provide linear hydraulic movement with a controlled speed for various loads such as no-load and 5100 N, with a constant oil temperature. To achieve this study, a fluid power control system was designed.

2.1. Component of the Hydraulic System

The system contains a fluid power supply unit, which provides the required flow rate at a specific supply pressure; p_s to a hydraulic cylinder through a servo control valve or a proportional directional flow control valve (PV) to study its effect on system performance. The oil reservoir and piping of the unit are designed according to standard specifications. The heating and cooling units are connected to keep the temperature constant. Fig. 1 demonstrates a block diagram of the fluid power control system.

The pump rotational velocity can be changed using a frequency inverter as an input signal to vary the output of the electrical motor. The flow rate and direction are controlled using a servo control valve operated by an electronic amplifier using a potentiometer or a proportional directional flow control valve operated through two directional forward and backward switches. Therefore, the displacement of the hydraulic linear actuator can be controlled.

2.1.1. Fluid Power Supply Unit

The fluid power supply unit fed the control system with fluid with a controlled flow rate and pressure. The system consists of an electric motor (7.5 kW) and a fixed displacement hydraulic gear pump, which produces fluid at a maximum rate of 30 L/min under pressure to the actuator. The supply pressure, p_s is changed from 10 to 50 bar, and the flow rate is controlled by the value of the

electric signal to the flow control valves. The supply unit contains an oil reservoir with accessories, such as a temperature indicator and oil level, in addition to a pressure relief valve, check valve, accumulator, and filters. The oil used in the system of this investigation was of type CO-OP Hydraulic 4 ISO VG 68. The working oil temperature of the system was 30 ºC. The hydraulic fluid power control circuit is shown in Fig. 2.

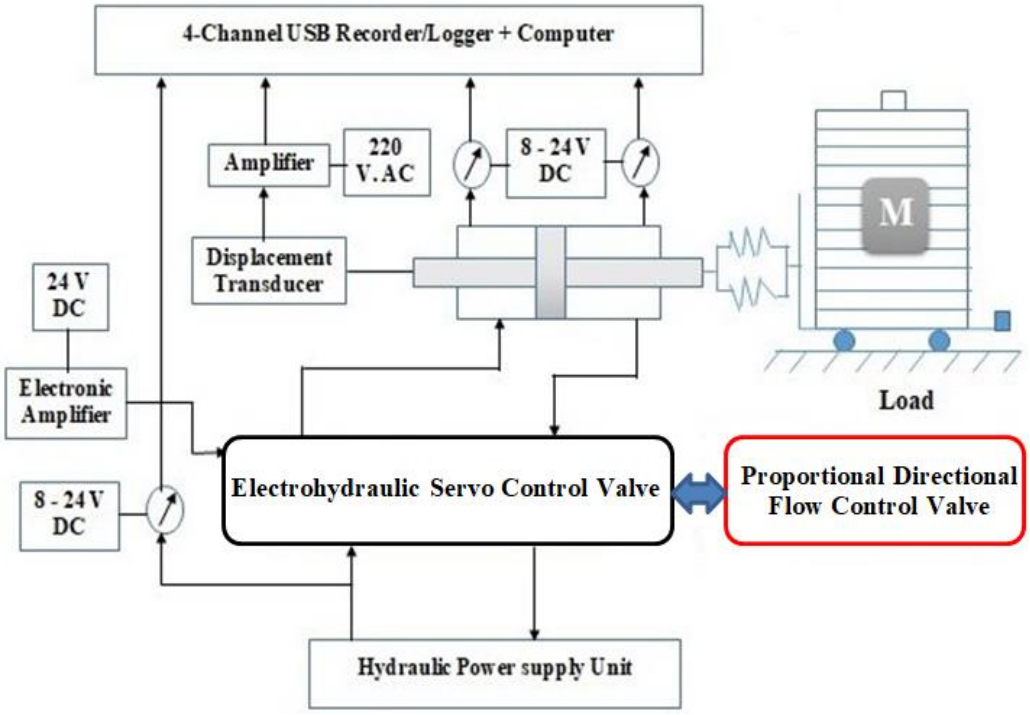

Fig. 1. Block diagram of a fluid power control system

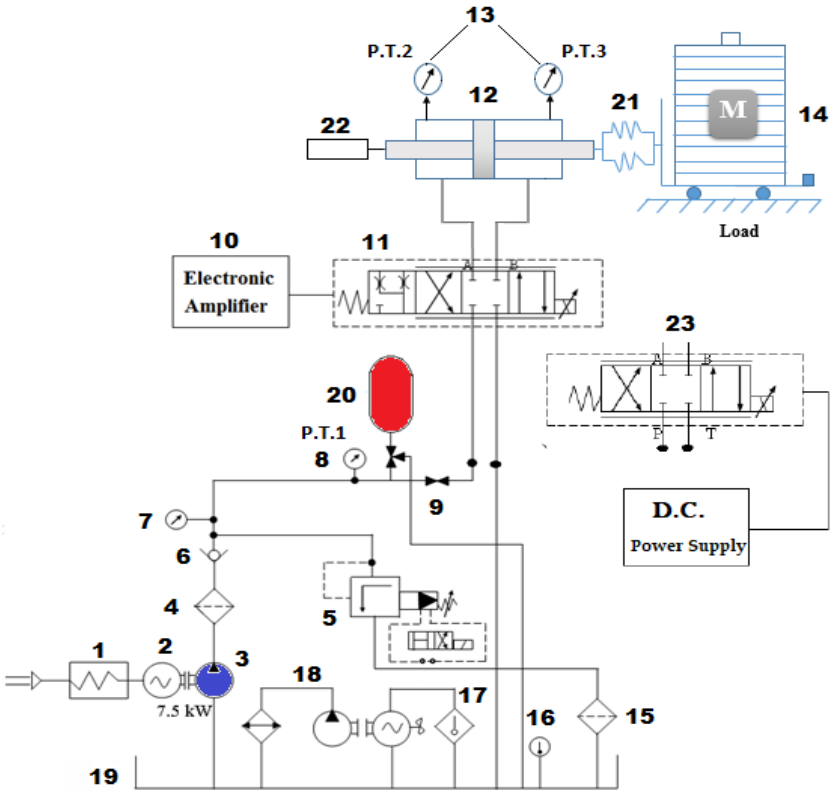

Fig. 2. Hydraulic circuit of the fluid power control system

1: Inverter 2: Electric motor 3: Gear pump 4: Pressure filter 5: Pilot Operated Pressure Relief Valve 6: Non return valve 6: Manometer. 250 bar 8: Pressure transducer, 100 bar 9: Shut: Off valve 10: Electronic amplifier 11: Servo Control valve 12: Hydraulic cylinder 13: Pressure transducer, 50 bar 14: loads 15: Return filter 16: Fluid level and temperature gauge 17: Thermostst and heating unit 18: Cooling unit 19: Oil reservoir, 110 L 20: Accumulator 21: Springs 21: Displacement transducer 23: Proportional directional control valve.

2.1.2. Cooling Power

The oil temperature affects its viscosity. Variations in oil viscosity during system operation affect the system performance. Therefore, it is important to maintain the oil temperature constant during system operation to maintain the oil viscosity constant. Since the oil temperature increases during system operation, a cooling unit should be attached to the system. According to the conductivity lows, the cooling power can be calculated as:

$$P = C_h * A_T * \Delta T \quad (1)$$

Where,

P = cooling power; [W]

C_h = thermal conductivity coefficient; [kcal. /m^2 .hr. ^oC]

A_T = tank surface area; [m^2]

ΔT = temperature difference; [^oC]

Hence, a cooling unit could be designed. The unit also includes a heating unit for the system's initial operating duration, as well as a thermostat to control the on/off times of the cooling/heating elements to maintain a steady temperature throughout the system.

2.1.3. Frequency Inverter

The frequency inverter is used to control the speed of the electrical AC motor to control the supply pressure and flow rate of the hydraulic pump. The fluid power supply unit was calibrated by changing the input signal to the frequency inverter and measuring the output supply pressure; p_s of the hydraulic pump using a manometer and Digibar pressure transducer. Fig. 3 shows a block diagram of the fluid power supply unit.

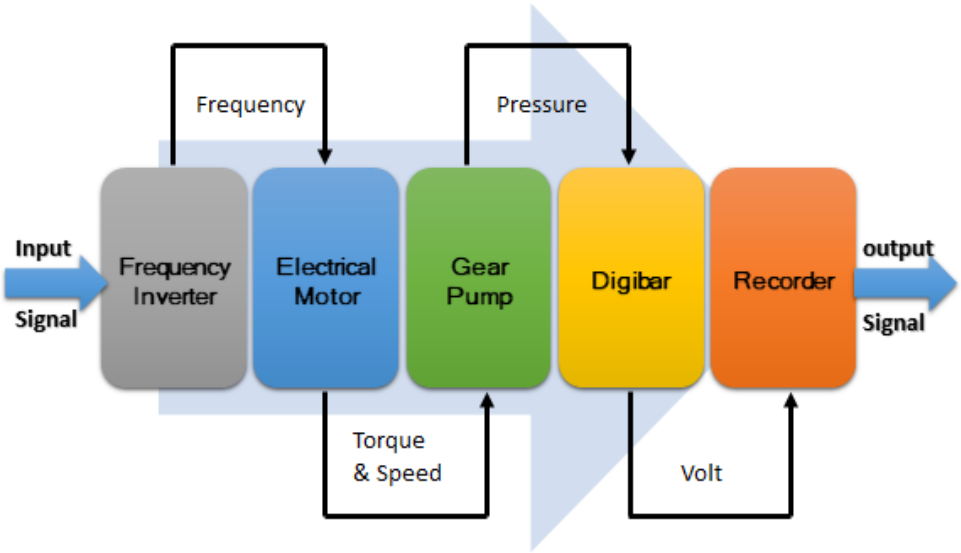

Fig. 3. Block diagram of the supply pressure calibration process

2.1.4. Servo Control Valve

An electro-hydraulic servo control valve was used in this investigation. a schematic of the valve is shown in Fig. 4.

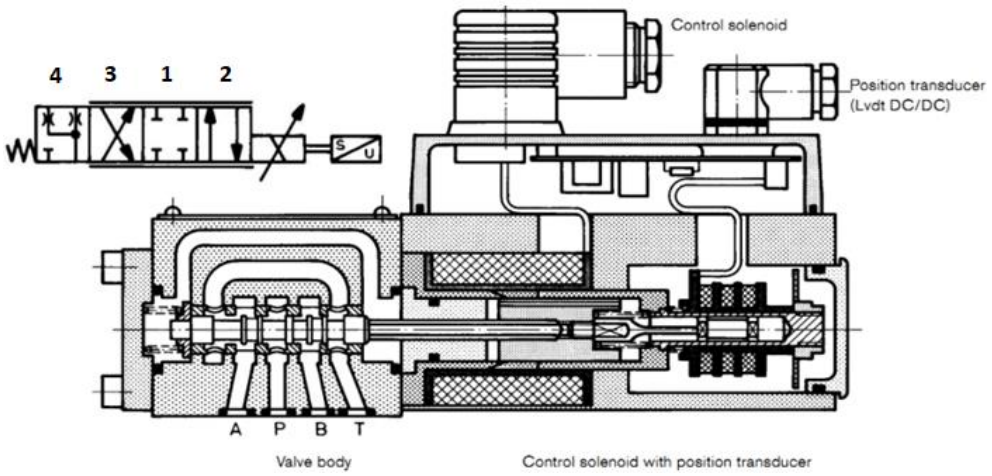

Fig. 4. Symbol and schematic drawing of the servo control valve

This valve is a Bosch servo solenoid valve; it is an electro-hydraulic continuous-action valve that is directly controlled with integrated control electronics. The spool position sensor is of the LVDT type. It is developed from proportional directional flow control valves. It is in no way inferior to a servo valve in terms of the static and dynamic performances. The flow rate of the valve is 40 l/min, with a nominal pressure drop of 35 bar, and a maximum pressure of 315 bar. The valve amplifier card which is compatible with the proportional valve, is powered by 24-volt DC with a maximum current of 1.5 A. The valve command signal is in the range of ±10 V. As it is a continuous action valve, an important requirement for its use is zero-lap in the mid-position area. A zero-lap orifice requires high manufacturing precision and hard-wearing materials.

2.1.5. Proportional Directional Flow Control Valve

The flow control valve was chosen as a 4/3 proportional pilot-operated valve. This type is a 4-way valve operated by proportional solenoids. The valve type is: REXROTH 4WRZ 10 W 50-40. It is a closed-canter, overlapped spool valve design. This value was used to compare the servo-control valve performance in the same investigation. A schematic of the valve is shown in Fig. 5.

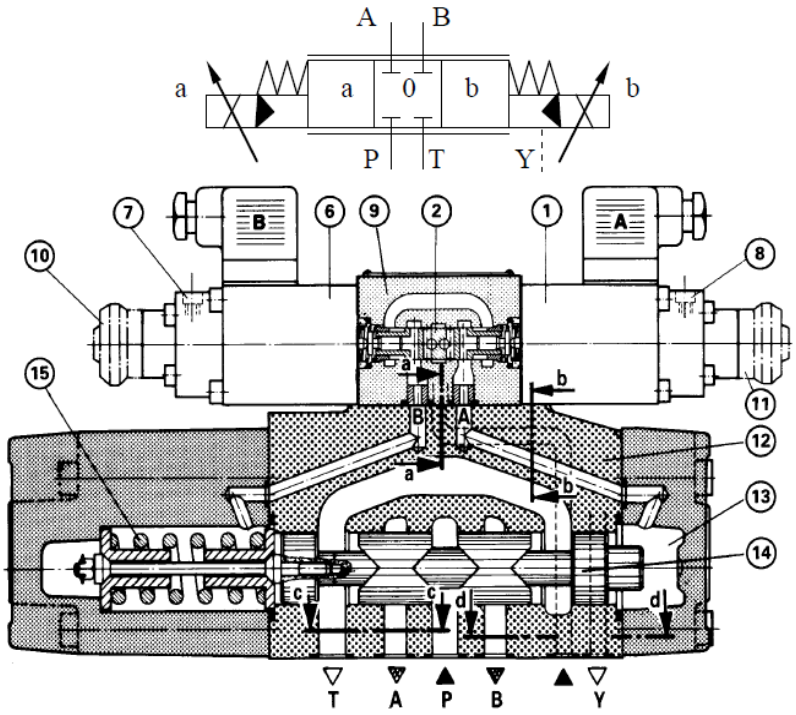

Fig. 5. Symbol and schematic drawing of proportional directional flow control valve

2.2. Measurement Devices and Calibration

An inductive displacement transducer is used to measure the piston displacement in the hydraulic cylinder. Pressure Digibar transducers are used to measure the inlet and outlet pressure values. A four-channel USB recorder/logger was used to convert the received voltage and current signals from the transducers to the computers to be evaluated.

2.2.1. Transducers Calibration

This section discusses how to calibrate the transducers used in the experimental setup. The pressure transducers are calibrated by measuring various pressure values and recording the corresponding voltage using a 4-channel USB recorder/logger. The flow rate of the system was calibrated using the bucket-stop-watch technique to measure the output flow rate of the control valves. The displacement transducer was calibrated by pushing the plunger a known distance and measuring the resulting voltage. A calibration curve is then generated to determine the relationship between the distance traveled and the received voltage.

3. Experimental Procedures

In this experimental investigation, the performance of a linear hydraulic control system was studied using an electrohydraulic servo control valve (SV) and a proportional directional flow control valve (PV). The system was designed to measure variations in the system supply pressure and the pressure response in the two chambers of the hydraulic actuator during piston movement.

The displacement, velocity, and flow rate of the piston were experimentally evaluated under various operating conditions, including supply pressures of 10, 20, 30, 40, and 50 bar, system stiffness's of 0.0, 18, and 32 N/mm, temperature of 30°C, and loads of no-load and 5100 N.

3.1. Methods of Conducting Experiments

A system was built to run the experiments in real-time. In this experimental investigation, an electrohydraulic servo control valve (SV) was connected to the hydraulic system, and the experiment was conducted. Then the system was disconnected, the proportional directional flow control valve (PV) was connected, and the experiment was repeated. The performance of the system was studied using hydraulic actuator. Fig. 6 and Fig. 7 show photographs of the system under investigation.

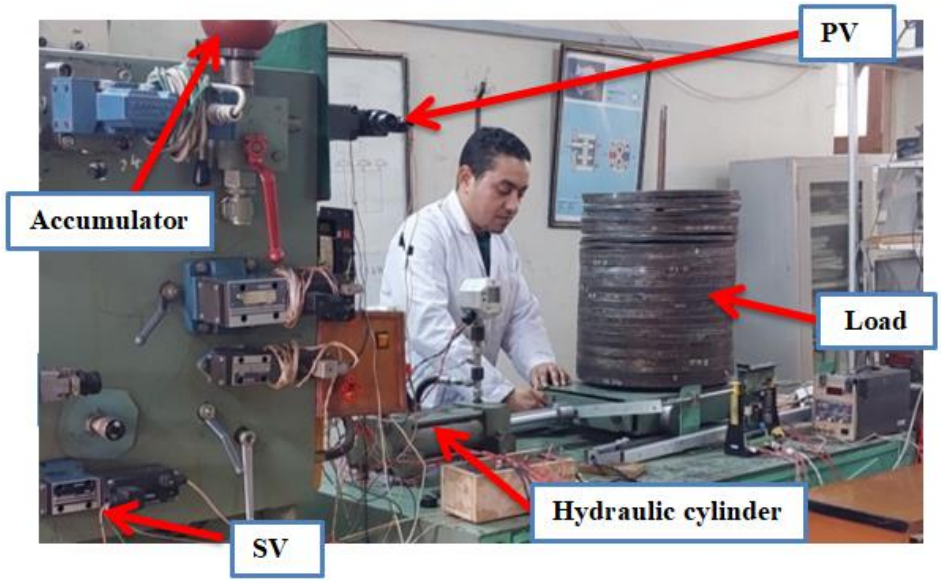

Fig. 6. Front photograph of the linear hydraulic control system

First, we studied the effect of valve flow rate at full opening. Second, the actual supply pressure-decay; p_{sa} has been recorded for different values of the supply pressure p_s. Finally, to study the effect

of the loading system on the performance, experiments were carried out under no-load condition when connecting either the SV or the PV. The system was loaded with 5100 N.

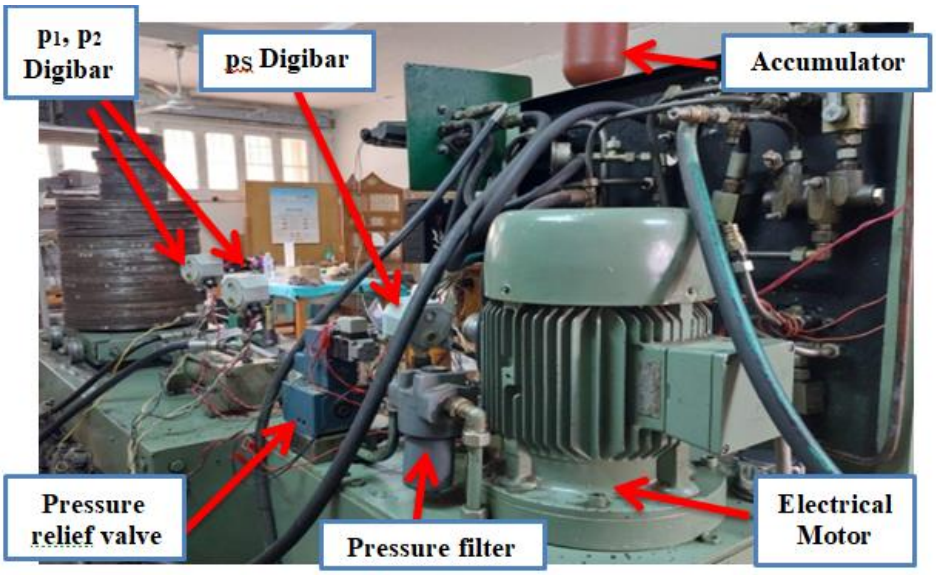

Fig. 7. Photograph of the rear view of the linear hydraulic control system

3.2. Control Valves Performance

The performances of both the SV and PV were investigated by measuring the output flow in 1 minute according to a specific value of the input voltage signal to the solenoid of the valves under a specific value of the supply pressure.

The servo control valve receives an electrical signal from a DC power supply through an electronic amplifier card and a 10 kΩ potentiometer. The 10 kΩ potentiometer is used to adjust the desired displacement and speed of the hydraulic cylinder piston. The proportional valve (PV) receives an electrical signal from a power supply through two directional forward and backward switches, which control the direction of the hydraulic cylinder.

3.3. Statistical Methods

In this study, after accumulating the measured data from all the tests, the difference between the data for the two hydraulic valves was established as an objective function. The paired t-test was used to evaluate significant differences in the SPSS program.

4. Results and Evaluation

The performance of the spool valve, the flow force effect, and the supply pressure decay during system operation are discussed. The effect of stroke period on the static and dynamic performance is investigated.

The results of the experimental work are compared. The comparison is made in the case of connecting the proportional directional flow control valve and the servo flow control valve.

4.1. Evaluation of System Flow Rate

The system performance was evaluated by the relationship between the flow rate; Q versus valve opening. A comparison of the two system designs at p_s = 50 bar under no load is given by Table 1. Furthermore is illustrated in Fig. 8.

The paired t-test p-value indicates a significant difference between the SV and PV systems in terms of the flow rate and valve opening percentage. The result show that SV systems consistently

generate higher flow rates than PV systems at all valve-opening percentages. Furthermore, there is a strong positive relationship between valve opening and flow rates in both the SV and PV systems. These data highlight the effectiveness of the SV systems in terms of high flow rates.

Table 1. Variation of system flow rate; Q about valves-opening Φ_s and Φ_p; for supply pressure; ps = 50 bar under no-load conditions at T = 30 ^{O}C

valve opening; Φ [%]	SV flow rate; Q [mL/s]	PV flow rate; Q [mL/s]
10	47.51	31.90
30	78.03	64.80
50	84.84	71.85
80	89.47	73.98
100	91.33	75.00

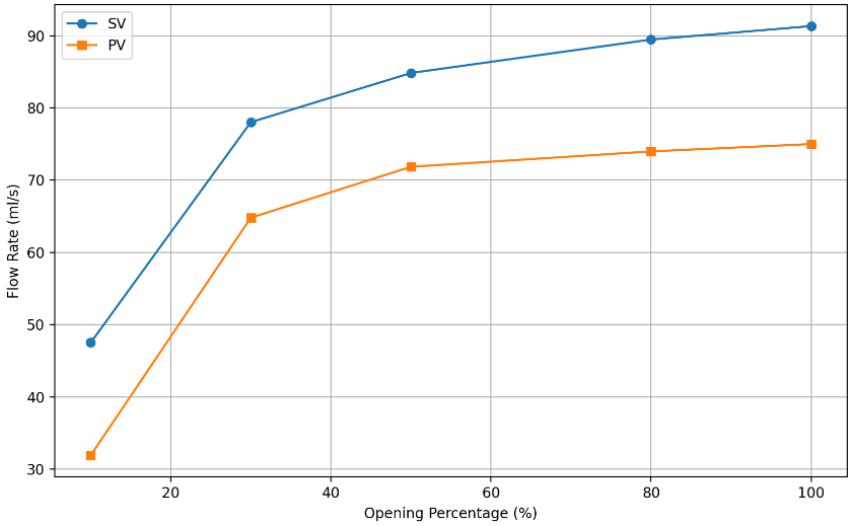

Fig. 8. Variation of system flow rate; Q about valves-opening (Φ_s) to (Φ_p); for supply pressure; p_s = 50 bar under no-load conditions at T = 30 ^{O}C

For illustration, at a supply pressure of 50 bar and no-load circumstances of 30°C, the SV's flow rate at full opening is 91.33 mL/s, whereas the PV system delivers 75 mL/s. Fig. 9 and Table 2 show that the SV design improved the flow rate by 21.77% compared to the PV design.

Table 2. Comparison of the system flow rate; Q for the two systems designs SV and PV for supply pressure; p_s = 50 bar under no-load

System designs	SV	PV
Flow Rate Q; [mL/s]	91.33	75
Improvement of Servo Flow rate; [%]	21.77 %	

Due to the zero-lap configuration between the spool land and the valve body ports of the servo control valve, even minor spool displacement causes the flow to occur immediately. As a result, the hydraulic actuator responds faster to any control signal.

A higher flow rate allows the actuators to move faster, thereby increasing the system efficiency. This characteristic is critical for high-speed applications, such as robotic arms and hydraulic presses. However, in applications that require precision control, such as aerospace, a balanced flow rate provides exact movement.

4.2. Evaluation of System Supply Pressure Decay

The supply pressure decays differently when the SV or PV is connected. A comparison of the two cases is achieved. The percentage of the actual supply pressure to the initial value of the supply pressure p_{sa}/p_s is calculated for both cases in Table 3 furthermore, plotted in Fig. 10.

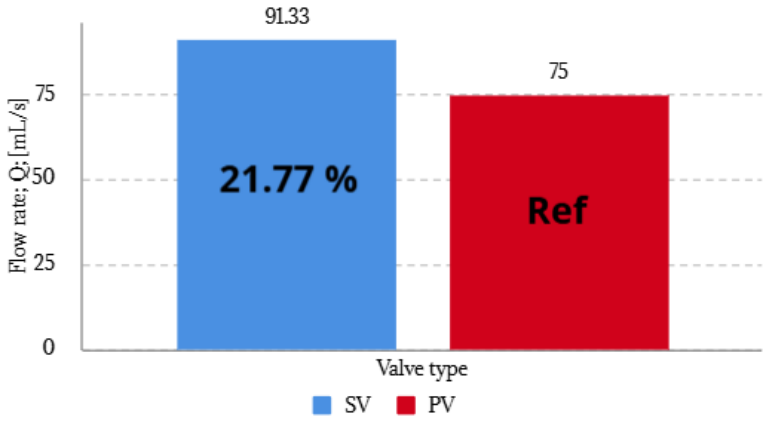

Fig. 9. Improvement of servo flow rate; [%]

Table 3. Pressure ratio; p_{sa}/p_s for different system cases at maximum flow rate and under no-load

p_s; [bar]	Pressure ratio p_{sa}/p_s; [%]	
	SV	PV
10	61.518800	61.884310
20	46.876275	42.509520
30	44.532567	36.500160
40	40.911600	33.903425
50	38.507220	32.385120

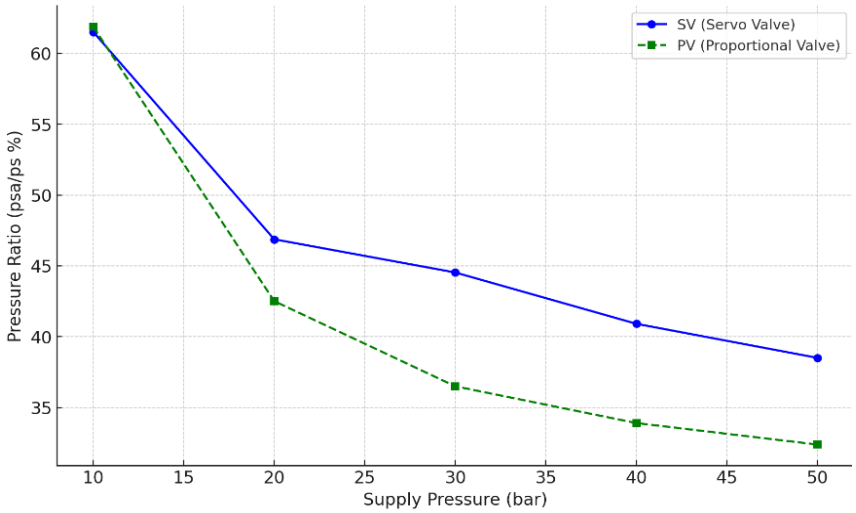

Fig. 10. Pressure ratio; psa/ps for SV and PV at T = 30 ºC, maximum flow rate, under no-load

The statistical examination of the pressure ratios at various pressure levels demonstrates that the pressure ratios for both the SV and PV systems consistently decrease as the pressure increases. Paired t-tests revealed statistically significant differences in the pressure ratios between the SV and PV systems at lower pressure levels, as shown by p-values less than the 0.05. These results show that SV systems are more efficient at pressure retention than PV systems.

The comparison of the results of this investigation in the case of connecting the SV to that in the case of connecting PV, declared that the actual supply pressure in the case of the SV at 30 ºC and p_s = 50 bar is 19.25 bar, and in the case of the connecting PV is 16.19 bar. This illustrates that by connecting the servo control valve there is an improvement in the value of the actual supply pressure by 18.90 % as shown in Fig. 11.

Pressure decay can slow actuator movement, resulting in increased cycle times and lower productivity, particularly in industrial automation and construction. Thus, assessing and managing

pressure decay is critical for ensuring constant performance and safety in hydraulic systems, especially in high-demand applications.

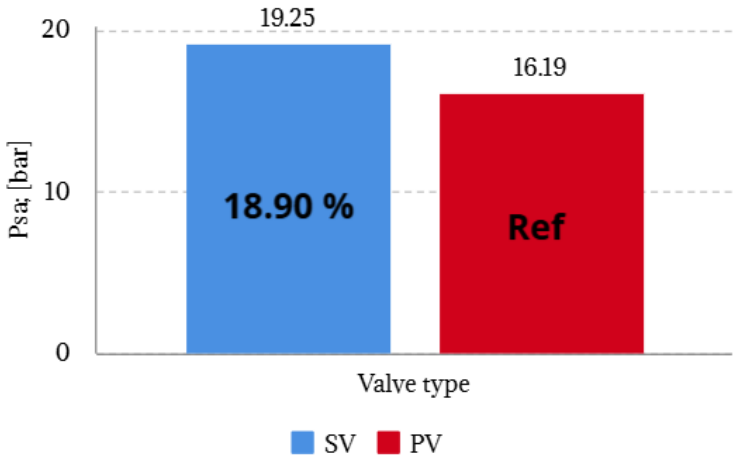

Fig. 11. Percent increase in the actual supply pressure at p_s = 50 bar due to variation in the system valve design

4.3. Effect of System Design on the Stroke Period

The effect on the system dynamics is determined when either the SV or PV is connected to the hydraulic. Comparison of the two system designs for p_s = 10, 20, 30, 40, and 50 bar at no-loading is recorded in Table 4 furthermore is illustrated in Fig. 12.

Table 4. Comparison of stroke period to SV and PV for different supply pressure values under no-load and without springs

Supply pressure; p_s[bar]	SV stroke period; t [sec]	PV stroke period; t [sec]	Improvement
10	59.6	98.5	40%
20	32.6	37.5	13%
30	22.3	24	7%
40	17.2	17.6	2%
50	13.6	13.8	1.5%

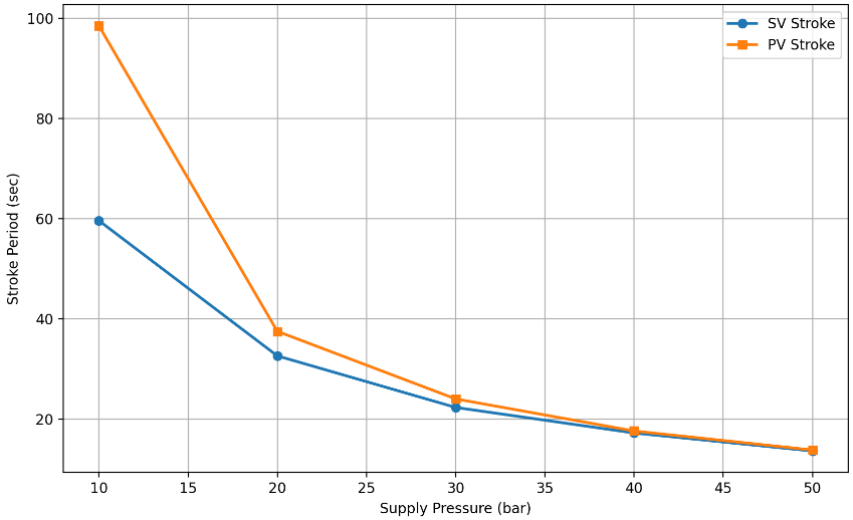

Fig. 12. Relationship between stroke period and supply pressure for both the SV and PV at no-load and without spring stiffness

It could be remarked that from Table 4, the stroke period in the case of connecting the SV or PV has a slight difference in values at the same stroke distance, specifically at high supply pressure;

p_s = 50 bar. But at the low values of supply pressure; p_s = 10 bar, the values of the stroke period values differ between the two system designs. The stroke period values in the case of connecting the SV are less than 40 % in the case of connecting the PV. The relationship is inverted between supply pressure and the Stroke period. Maintaining a proper ratio of the pressure and stroke period is critical in precision applications, such as robotics, to achieve accurate and controlled motions.

4.4. Effect of Temperature on Stroke Period

The relationship between supply pressure; p_s = 10, 20, 30, 40, and 50 bar at full stroke and stroke period (t) is used to evaluate the system dynamics of stroke period performance. Comparison of the three conditions of operation temperature; T = 30, 40, and 50 ºC under no-load conditions without springs in the case of the connecting SV. The experimental data were extracted from Table 5 furthermore, plotted in Fig. 13.

Table 5. Variation in the system stroke period; t to the variation of supply pressure; ps under load; W = 0.0 N, without stiffness; K furthermore, temperature conditions

Supply pressure; p_s [bar]	Stroke period; t [sec] at T = 30 ºC	Stroke period; t [sec] at T = 40 ºC	Stroke period; t [sec] at T = 50 ºC
10	54.60	40.90	33.80
20	26.30	20.10	16.90
30	18.10	13.80	12.20
40	13.40	10.50	9.20
50	10.90	8.40	7.60

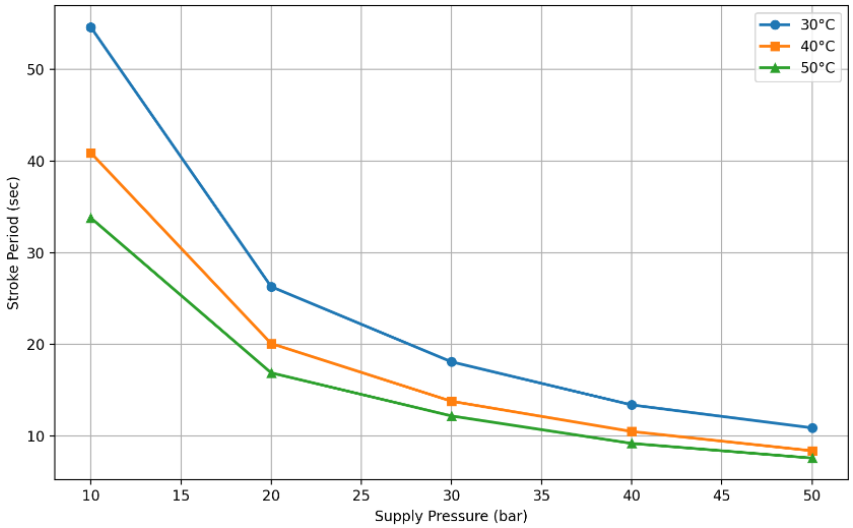

Fig. 13. Variation in the system stroke period; t in relation to the supply pressure at temperature values; T = 30, 40, and 50 ºC

Paired t-tests revealed a significant difference in stroke duration between 30°C and 40°C (p = 0.045) and a marginally significant difference between 30°C and 50°C (p = 0.052). These data imply that pressure and temperature have a major impact on stroke duration, with greater pressures and temperatures typically resulting in shorter stroke durations. This suggests that ideal operating conditions can be achieved by carefully controlling both parameters. The percentage stroke time for 50 bar was calculated for the temperature range and is presented in Table 6 and plotted in Fig. 14.

Table 6. Comparison of stroke period; t for the temperature is operating conditions at T = 30, 40, and 50 ºC for supply pressure; p_s = 50 bar under no load without springs at full stroke

Temperature; T [º C]	30 ºC	40 ºC	50 ºC
Decreasing percentage of stroke time; [%]	Ref.	21.34 %	41.17 %

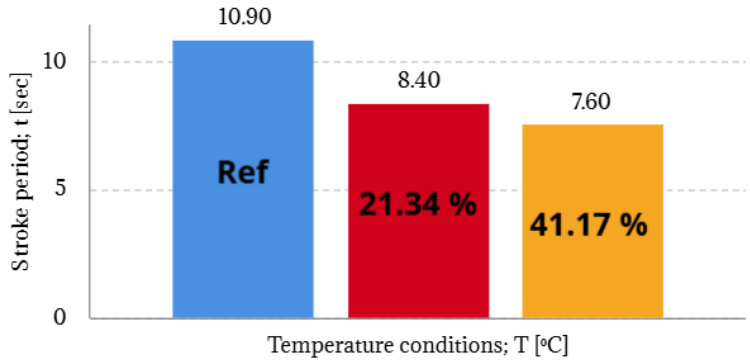

Fig. 14. Relationship between system stroke period; t to temperature conditions; T = 30, 40, and 50 °C at supply pressure; p_s = 50 bar

According to Table 6 and Fig. 14, the stroke period decreases as the temperature and supply pressure increase to achieve the same stroke distance. This occurs because the oil viscosity decreases. Hence, higher power from the motor and pump is required to achieve the same pressure. Accordingly, with this higher power, the piston of the hydraulic cylinder moves faster than that at low temperatures.

4.5. Effect of Load on System Dynamics

According to the present experimental investigation, system loading affects the dynamic performance. The operating condition of the fluid power control system is investigated. This section discusses the effects of applying a 5100 N load to different system designs. The results are presented in Table 7 and plotted in Fig. 15.

Table 7. Relationship between stroke periods; t and supply pressure; p_s under load; W = 5100 N

Supply pressure; p_s [bar]	SV Stroke period; t [sec]		PV Stroke period; t [sec]	
	W = 0.0 N	W = 5100 N	W = 0.0 N	W = 5100 N
10	59.60	63.10	98.50	103.30
20	32.60	31.80	37.50	38.50
30	22.30	22.70	24.00	24.70
40	17.20	16.60	17.60	18.00
50	13.60	13.80	13.80	14.30

The T-test findings showed no statistically significant difference between the stroke periods of the SV and PV valves under the each load condition (0.0 N or 5100 N), as evidenced by the p-values of 0.62 and 0.60, respectively. This indicates that, under the specified experimental conditions, the valve type has no significant effect on the stroke period when the supply pressure and load are changed. These results suggest that the SV and PV valves function similarly under various load conditions. Future studies should consider other factors or extended settings to further confirm these results, particularly when applying large loads greater than 5100 N.

According to Table 7 and Fig. 15 at low supply pressures when the system is loaded, the system requires more power to move the actuator. This higher power requirement indicates that the system may require more time to get over the load's inertia and resistance, resulting in longer stroke duration. Larger loads often result in longer system response times because hydraulic actuators require more force and time to reach the desired position. This may result in control latency or poor performance in fast-paced systems, including manufacturing automation.

4.6. Dynamics Performance of Different Hydraulic Control System Design

This experimental work investigates the effect of the system valve type on the dynamic performance of a fluid power control system. During this investigation, the effect of connecting each of the two different valves to the hydraulic control system on the dynamic was studied. Data are

shown in Table 8 and Table 9 under no-load conditions, without springs, and temperature; T = 30 ^{O}C at different supply pressure; p_s = 10, 20, 30, 40, and 50 bar when connecting the SV or PV to the hydraulic actuator. Results are registered in Table 8 and Table 9.

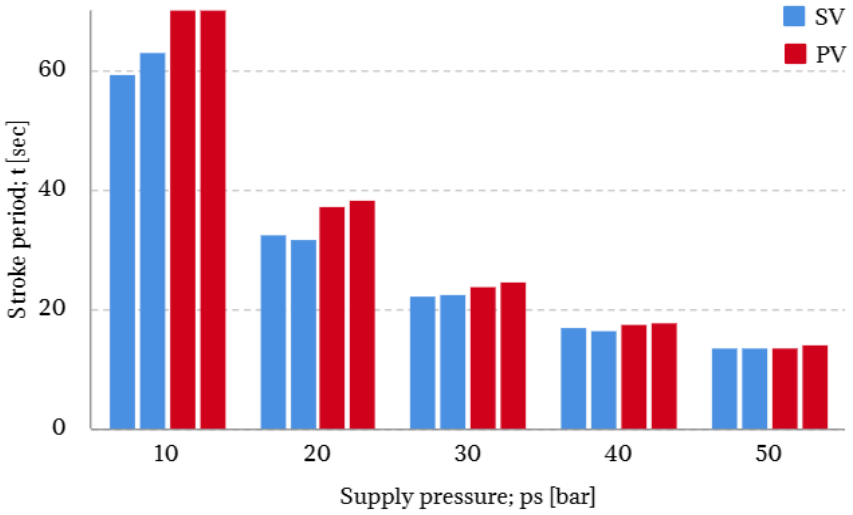

Fig. 15. Relationship between stroke periods; t and supply pressure under load; W = 5100 N

The corresponding percentage and in dB for displacement amplitude are calculated and registered in the same Table. Semi-log charts of the amplitude versus frequency plots are shown in Fig. 16 and Fig. 17. Comparing the results in Table 8 to those in Table 9 for the same operating conditions of load, supply pressure, and temperature, it could be recognized that the frequency of piston displacement decreases with connecting PV more than SV at low values of supply pressure, but it differs slightly at high values of supply pressure for the two system designs. To discuss the effect of system design, for connecting each one of the two different valves on the bandwidth frequency of the system, the bandwidth values were extracted at -3 dB from the dynamic curves in Fig. 16 and Fig. 17 at different supply pressure values, presented in Table 10, and plotted in Fig. 18 and Fig. 19.

Table 8. Variation in the system displacement amplitude and frequency under no-load, without springs at temperature; T = 30 ^{O}C versus different supply pressure values with SV connection

p_s, [bar]	SV			Amplitude		
	Stroke	Time of Stroke; t [sec]	Frequency; *f*; 1/t [Hz]	|X|	X [%]	X [dB]
10	Full	59.60	0.016779	185	100	0
	3/4	44.70	0.022371	138.75	75	- 2.498775
	1/2	29.80	0.033557	92.50	50	- 6.020600
	1/4	14.90	0.067114	46.25	25	- 12.041200
20	Full	32.60	0.030675	185	100	0
	3/4	24.45	0.040899	138.75	75	- 2.498775
	1/2	16.30	0.061350	92.50	50	- 6.020600
	1/4	8.15	0.122699	46.25	25	- 12.041200
30	Full	22.30	0.044843	185	100	0
	3/4	16.75	0.059702	138.75	75	- 2.498775
	1/2	11.15	0.089686	92.50	50	- 6.020600
	1/4	5.58	0.179212	46.25	25	- 12.041200
40	Full	17.20	0.058140	185	100	0
	3/4	12.90	0.077519	138.75	75	- 2.498775
	1/2	8.60	0.116279	92.50	50	- 6.020600
	1/4	4.30	0.232558	46.25	25	- 12.041200
50	Full	13.60	0.073529	185	100	0
	3/4	10.20	0.098039	138.75	75	- 2.498775
	1/2	6.80	0.147059	92.50	50	- 6.020600
	1/4	3.40	0.294118	46.25	25	- 12.041200

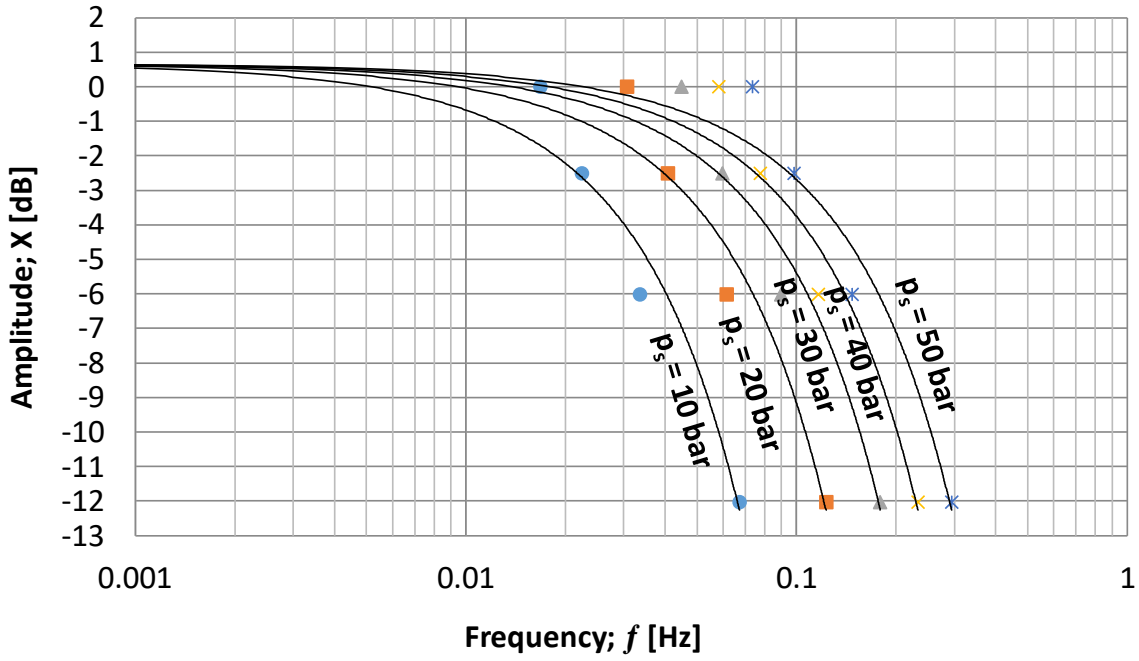

Fig. 16. Relationship of system amplitude; X versus frequency; f for supply pressure; p_s = 10, 20, 30, 40, 50 bar under no-load conditions, without springs and T = 30 ^{O}C with SV connection

Table 9. Variation in the system displacement amplitude and frequency under no-load, without springs at temperature; T = 30 ^{O}C versus different supply pressure values with PV connection

p_s, [bar]	PV			Amplitude		
	Stroke	Time of Stroke; t [sec]	Frequency; f; 1/t [Hz]	|X|	X [%]	X [dB]
10	Full	98.50	0.010152	185	100	0
	3/4	74.00	0.013514	138.75	75	- 2.498775
	1/2	49.25	0.020305	92.50	50	- 6.020600
	1/4	24.65	0.040568	46.25	25	- 12.041200
20	Full	37.50	0.026667	185	100	0
	3/4	28.00	0.035714	138.75	75	- 2.498775
	1/2	18.75	0.053333	92.50	50	- 6.020600
	1/4	9.35	0.106952	46.25	25	- 12.041200
30	Full	24.00	0.041667	185	100	0
	3/4	18.00	0.055556	138.75	75	- 2.498775
	1/2	12.00	0.083333	92.50	50	- 6.020600
	1/4	6.00	0.166667	46.25	25	- 12.041200
40	Full	17.60	0.056818	185	100	0
	3/4	13.20	0.075758	138.75	75	- 2.498775
	1/2	8.80	0.113636	92.50	50	- 6.020600
	1/4	4.40	0.227273	46.25	25	- 12.041200
50	Full	13.80	0.072464	185	100	0
	3/4	10.35	0.096618	138.75	75	- 2.498775
	1/2	6.90	0.144928	92.50	50	- 6.020600
	1/4	3.45	0.289855	46.25	25	- 12.041200

Table 10. System bandwidth frequency under different valve-type conditions

Supply pressure; p_s[bar]	SV Bandwidth; Ɓ [Hz]	PV Bandwidth; Ɓ [Hz]]	Improvement
10	0.025	0.015	65 %
20	0.045	0.039	15 %
30	0.066	0.061	8 %
40	0.085	0.083	3 %
50	0.108	0.106	1.5%

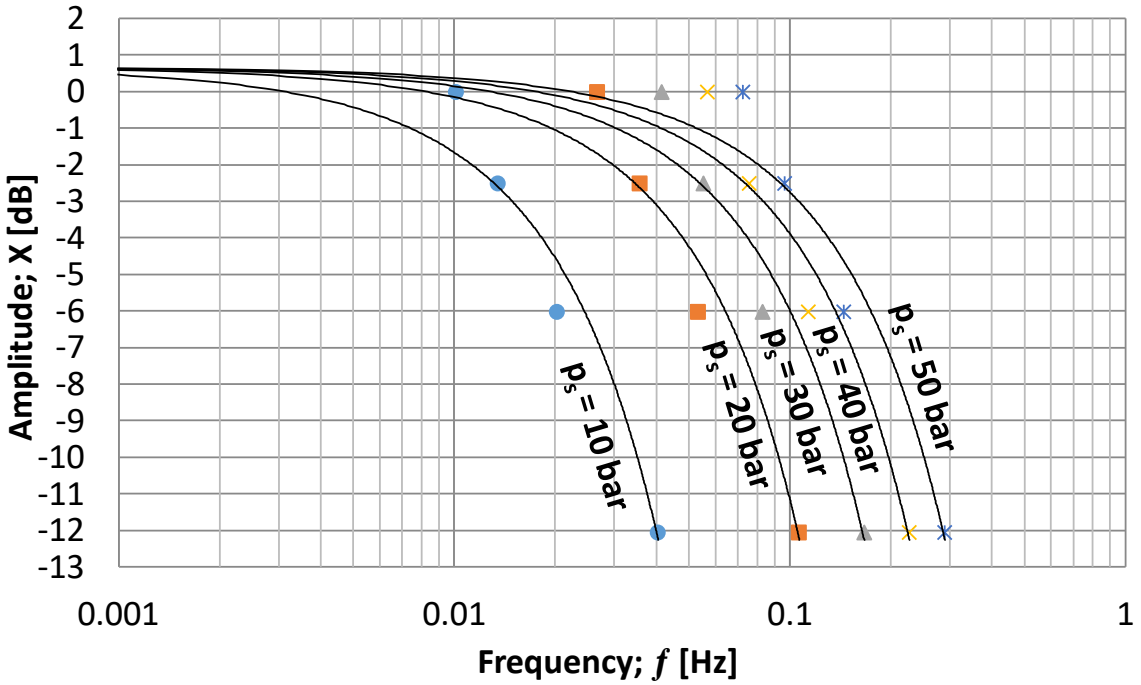

Fig. 17. Relationship of system amplitude; X versus frequency; f for supply pressure; p_s = 10, 20, 30, 40, 50 bar under no-load conditions, without springs and T = 30 ^{O}C with PV connection

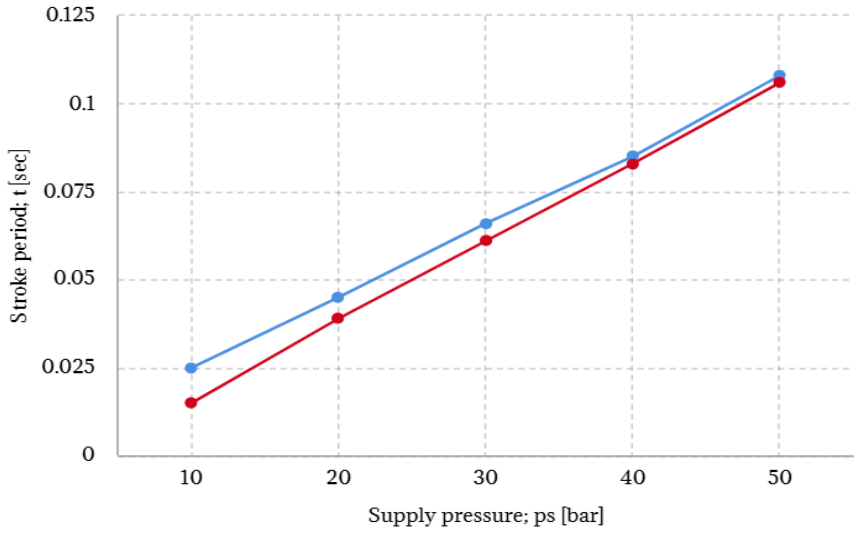

Fig. 18. Relation between bandwidth frequencies and Supply pressure at temperature; T = 30 OC under no-load conditions and without springs

The statistical study demonstrated substantial variation in bandwidth characteristics between the SV and PV systems (paired t-test p-value = 0.028), showing separate performance patterns for the two valve types. Both systems exhibit an important beneficial relationship between bandwidth and supply pressure.

Fig. 18 and Fig. 19 show that the bandwidth frequency of the system in the case of connecting the SV at lower values of supply pressure is 65% higher than in the case of connecting the PV, but at high values of supply pressure, the bandwidth differs slightly. In hydraulic valves, bandwidth refers to the frequency range the valve can efficiently regulate fluid flow and, by extension, actuator movement. Greater bandwidth means that the valve can respond faster to changes in the control signal, thereby allowing more accurate and dynamic control. Therefore, the servo valve was defined by its fast response and high bandwidth.

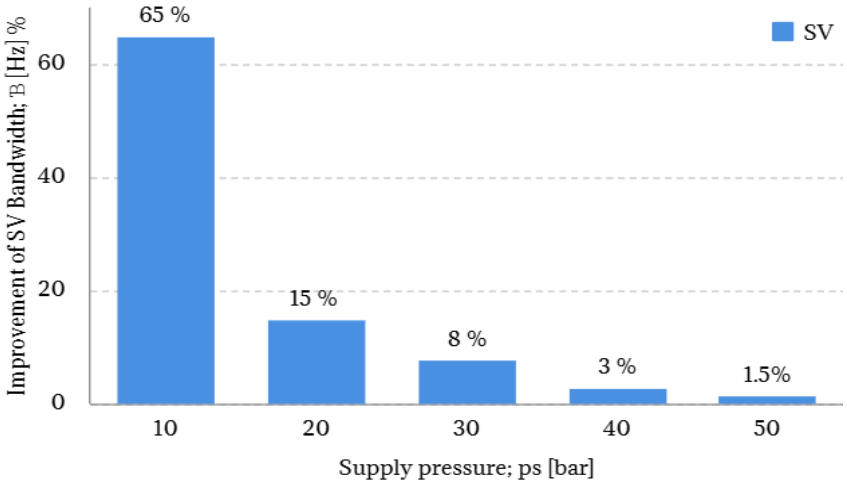

Fig. 19. Percentage of SV bandwidth improvement; [%]

4.7. Comparison with Previous Studies

Energy-saving solutions to hydraulic control systems have significantly advanced in response to the growing demand for efficient control systems in various industrial applications. Recent research has highlighted the control strategies and system designs that influence energy use. When comparing two types of hydraulic control valves, connecting a servo control valve enhances the system performance in terms of the flow rate and pressure decay. Servo hydraulic control valves can enhance the hydraulic system energy efficiency by accurately controlling the flow and pressure, lowering the pump demand, generating less heat, and reducing fluid loss. As a result, servo-hydraulic control valves play an important role in the establishment of energy-efficient hydraulic systems, thereby resulting in lower operational costs and a smaller environmental footprint.

5. Conclusion

This study investigates the static and dynamic performance of linear position control in a fluid power control system, with a focus on the effects of system design under various operating conditions. The SV and PV flow control valves were connected to the system for comparison. Connecting the SV results in a significant improvement in the system flow rate and actual supply pressure compared to the PV. At a supply pressure of 50 bar under no-load conditions, the flow rate improvement with SV was 21.77%. Additionally, the actual supply pressure is 18.90% higher with SV than with PV. The dynamic characteristics of the system, particularly the stroke period, show marked differences between the two e types of valves. At a supply pressure of 10 bar, the stroke period was 40% shorter for SV than for PV. However, this improvement decreases as the supply pressure increases. Piston displacement frequency is higher for SV than for PV, especially at low supply pressures. At a supply pressure of 10 bar, the bandwidth frequency of the SV is 65% higher than that of the PV. Hydraulic servo valve improvements such as higher flow rates, accurate pressure control, and quick responses enhance several of applications. These innovations result in higher output, reduced cycle times, increased safety, and lower operational costs. Hydraulic servo valves are thus becoming increasingly dependable and efficient, making them vital components in sectors such as aircraft, robotics, and manufacturing automation. The results provide useful information for determining the best valve type for various industrial applications based on the desired performance characteristics.

Further research could involve looking at various system designs by applying other control techniques, loading the system with a wide range of loads higher than 5100 N, exploring the performance of different types of valves, and studying the impact of compressibility on long-distance control systems.

Author Contribution: All authors contributed equally to the main contributor to this paper. All authors read and approved the final paper.
Funding: This research received no external funding.
Conflicts of Interest: The authors declare no conflict of interest.

Nomenclature

A_n	Nozzle flow [mm^2]
B	Bandwidth [Hz]
C_d	Discharge coefficient [%]
F	Frequency [Hz]
K	Spring stiffness [N/mm]
p_s	Supply pressure line [bar]
p_{sa}	Actual value of supply pressure [bar]
p_1, p_2	Cylinders inlet and outlet pressures [bar]
Δp	Pressure difference through valve opening [bar]
Q	System flow rate [L/min]
Q_n	Flow rate through valve nozzles [L/min]
T	Temperature [^{o} C]
T	Time [sec]
V	Command signal value [volt]
W	System load [N]
X	Piston stroke [dB]
X	Piston displacement [mm]
P	Oil density [kg/m^3]
Φ	Valve opening Percentage [%]
Φ_s	SV opening percentage [%]
Φ_p	PV opening percentage [%]

Abbreviations

A, B	Working lines
PV	Proportional directional flow control valve
SV	Electro hydraulic servo valve
DC	Direct Current
AC	Alternating Current

References

[1] L. W. Mays, "A very brief history of hydraulic technology during antiquity," *Environmental Fluid Mechanics*, vol. 8, no. 5-6, pp. 471-484, 2008, https://doi.org/10.1007/s10652-008-9095-2.

[2] S. Xu, C. M. Nunez, M. Souri, and R. J. Wood, "A compact DEA-based soft peristaltic pump for power and control of fluidic robots," *Science Robotics*, vol. 8, no. 79, p. eadd4649, 2023, https://doi.org/10.1126/scirobotics.add4649.

[3] C. R. Ortloff, "CFD Investigations of Water Supply and Distribution Systems of Ancient Old and New World Archaeological Sites to Recover Ancient Water Engineering Technologies," *Water*, vol. 15, no. 7, p. 1363, 2023, https://doi.org/10.3390/w15071363.

[4] A. Guran, "A fluid power actuation system for shape control of an elastic rod," *Engineering Mechanics 2022*, pp. 129-132, 2022, https://doi.org/10.21495/51-2-129.

[5] S. Y. Chien and M. S. Cramer, "Load and loss for high-speed lubrication flows of pressurized gases between non-concentric cylinders," *Journal of Fluid Mechanics*, vol. 867, pp. 1–25, 2019, https://doi.org/10.1017/jfm.2019.113.

[6] E. Franco and A. Astolfi, "Energy shaping control of underactuated mechanical systems with fluidic actuation," *International Journal of Robust and Nonlinear Control*, vol. 32, no. 18, pp. 10011–10028, 2022, https://doi.org/10.1002/rnc.6345.

[7] R. Dindorf, J. Takosoglu, and P. Wos, "Advances in Fluid Power Systems," *Energies*, vol. 14, no. 24, p. 8589, 2021, https://doi.org/10.3390/en14248589.

[8] H. H. Ali, A. W. Mustafa, and F. F. Al-Bakri, "A new control design and robustness analysis of a variable speed hydrostatic transmission used to control the velocity of a hydraulic cylinder," *International Journal*

of Dynamics and Control, vol. 9, no. 3, pp. 1078–1091, 2021, https://doi.org/10.1007/s40435-020-00716-w.

[9] Y. Yin, "Electro Hydraulic Control Theory and Its Applications Under Extreme Environment," *Elsevier*, 2019, https://doi.org/10.1016/C2016-0-04504-7.

[10] N. D. Manring and R. C. Fales, "Hydraulic Control Systems," *Wiley*, 2019. https://doi.org/10.1002/9781119418528.

[11] R. Ding, J. Zhang, B. Xu, M. Cheng, and M. Pan, "Energy efficiency improvement of heavy-load mobile hydraulic manipulator with electronically tunable operating modes," *Energy Conversion and Management*, vol. 188, pp. 447–461, 2019, https://doi.org/10.1016/j.enconman.2019.03.023.

[12] M. Papoutsidakis, A. Chatzopoulos, D. Papachristos, and C. Drosos, "Hydraulics and Pneumatics: Operational Characteristics and Control for Modern Industry Applications," *International Journal of Computer Applications*, vol. 178, no. 25, pp. 31–40, 2019, https://doi.org/10.5120/ijca2019919049.

[13] G. Wu, J. Yang, J. Shang, and D. Fang, "A rotary fluid power converter for improving energy efficiency of hydraulic system with variable load," *Energy*, vol. 195, p. 116957, 2020, https://doi.org/10.1016/j.energy.2020.116957.

[14] G. Wu, J. Yang, J. Shang, Z. Luo, T. Zou, and D. Fang, "On the Design of Energy-Saving Fluid Power Converter," *IEEE Access*, vol. 8, pp. 27769–27778, 2020, https://doi.org/10.1109/ACCESS.2020.2971669.

[15] K. Klinar, T. Swoboda, M. Muñoz Rojo, and A. Kitanovski, "Fluidic and Mechanical Thermal Control Devices," *Advanced Electronic Materials*, vol. 7, no. 3, pp. 1-20, 2021, https://doi.org/10.1002/aelm.202000623.

[16] J. Sun *et al*., "Self-powered In-Phase Sensing and Regulating Mechanical System Enabled by Nanogenerator and Electrorheological Fluid," *Advanced Functional Materials*, vol. 33, no. 9, p. 2212248, 2023, https://doi.org/10.1002/adfm.202212248.

[17] K. Liu, C. Zhang and Z. Sun, "Independent Pressure and Flow Rate Control Enabled by Hydraulic Free Piston Engine," *IEEE/ASME Transactions on Mechatronics*, vol. 24, no. 3, pp. 1282-1293, 2019, https://doi.org/10.1109/TMECH.2019.2906611.

[18] C. Wu, Z. Jiao, Y. Xu, C. Li, Q. Liu, and S. Wu, "Active control method for fluid borne noise in aerospace fluid systems of variable operation statuses," *Mechanical Systems and Signal Processing*, vol. 214, p. 111375, 2024, https://doi.org/10.1016/j.ymssp.2024.111375.

[19] R. Li *et al*., "Review of the Progress of Energy Saving of Hydraulic Control Systems," *Processes*, vol. 11, no. 12, p. 3304, 2023, https://doi.org/10.3390/pr11123304.

[20] A. Wiberg, L. Ericson, J. A. Persson, and J. Ölvander, "Additive manufacturing in fluid power with novel application to hydraulic pump design," *Proceedings of the Design Society*, vol. 4, pp. 1889–1898, 2024, https://doi.org/10.1017/pds.2024.191.

[21] F. Sciatti, P. Tamburrano, E. Distaso, and R. Amirante, "Digital hydraulic valves: Advancements in research," *Heliyon*, vol. 10, no. 5, p. e27264, 2024, https://doi.org/10.1016/j.heliyon.2024.e27264.

[22] Z. Tong *et al*., "Energy-saving technologies for construction machinery: a review of electro-hydraulic pump-valve coordinated system," *Journal of Zhejiang University-SCIENCE A*, vol. 21, no. 5, pp. 331–349, 2020, https://doi.org/10.1631/jzus.A2000094.

[23] P. Stump, N. Keller, and A. Vacca, "Energy Management of Low-Pressure Systems Utilizing Pump-Unloading Valve and Accumulator," *Energies*, vol. 12, no. 23, p. 4423, 2019, https://doi.org/10.3390/en12234423.

[24] B. Xu, J. Shen, S. Liu, Q. Su, and J. Zhang, "Research and Development of Electro-hydraulic Control Valves Oriented to Industry 4.0: A Review," *Chinese Journal of Mechanical Engineering*, vol. 33, no. 1, p. 29, 2020, https://doi.org/10.1186/s10033-020-00446-2.

[25] F. Sciatti, P. Tamburrano, P. De Palma, E. Distaso, and R. Amirante, "Detailed simulations of an aircraft fuel system by means of Simulink," *Journal of Physics: Conference Series*, vol. 2385, no. 1, p. 012033, 2022, https://doi.org/10.1088/1742-6596/2385/1/012033.

[26] P. Tamburrano *et al*., "Fuels systems and components for future airliners fuelled with liquid hydrogen," *Journal of Physics: Conference Series*, vol. 2385, no. 1, p. 012041, 2022, https://doi.org/10.1088/1742-6596/2385/1/012041.

[27] F. Sciatti, P. Tamburrano, E. Distaso, and R. Amirante, "Modelling of the Entire Aircraft Fuel System Through Simulink for Accurate Performance Evaluation," *ASME/BATH 2023 Symposium on Fluid Power and Motion Control, American Society of Mechanical Engineers*, 2023, https://doi.org/10.1115/FPMC2023-111795.

[28] Z. Jiao, H. Zhang, Y. Shang, X. Liu, and S. Wu, "A power-by-wire aircraft brake system based on high-speed on-off valves," *Aerospace Science and Technology*, vol. 106, p. 106177, 2020, https://doi.org/10.1016/j.ast.2020.106177.

[29] M. Cheng, Z. Han, R. Ding, J. Zhang, and B. Xu, "Development of a redundant anthropomorphic hydraulically actuated manipulator with a roll-pitch-yaw spherical wrist," *Frontiers of Mechanical Engineering*, vol. 16, no. 4, pp. 698–710, 2021, https://doi.org/10.1007/s11465-021-0646-2.

[30] R. Ding, M. Cheng, L. Jiang and G. Hu, "Active Fault-Tolerant Control for Electro-Hydraulic Systems With an Independent Metering Valve Against Valve Faults," *IEEE Transactions on Industrial Electronics*, vol. 68, no. 8, pp. 7221-7232, 2021, https://doi.org/10.1109/TIE.2020.3001808.

[31] P. Tamburrano, A. R. Plummer, E. Distaso, and R. Amirante, "A review of electro-hydraulic servovalve research and development," *International Journal of Fluid Power*, pp. 1–23, 2018, https://doi.org/10.1080/14399776.2018.1537456.

[32] P. Tamburrano, E. Distaso, A. R. Plummer, F. Sciatti, P. De Palma, and R. Amirante, "Direct Drive Servovalves Actuated by Amplified Piezo-Stacks: Assessment through a Detailed Numerical Analysis," *Actuators*, vol. 10, no. 7, p. 156, 2021, https://doi.org/10.3390/act10070156.

[33] H. Heinken, S. Ulrich, R. Bruns, and S. Schneider, "High-response electrorheological servo valve," *Journal of Intelligent Material Systems and Structures*, vol. 31, no. 2, pp. 297–307, 2020, https://doi.org/10.1177/1045389X19873427.

[34] P. Tamburrano, A. R. Plummer, E. Distaso, and R. Amirante, "A Review of Direct Drive Proportional Electrohydraulic Spool Valves: Industrial State-of-the-Art and Research Advancements," *Journal of Dynamics Systems, Measurement, and Control*, vol. 141, no. 2, p. 020801, 2019, https://doi.org/10.1115/1.4041063.

[35] R. Amirante, P. G. Moscatelli, and L. A. Catalano, "Evaluation of the flow forces on a direct (single stage) proportional valve by means of a computational fluid dynamic analysis," *Energy Conversion and Management*, vol. 48, no. 3, pp. 942–953, 2007, https://doi.org/10.1016/j.enconman.2006.08.024.

[36] R. Amirante, E. Distaso, and P. Tamburrano, "Experimental and numerical analysis of cavitation in hydraulic proportional directional valves," *Energy Conversion and Management*, vol. 87, pp. 208–219, 2014, https://doi.org/10.1016/j.enconman.2014.07.031.

[37] Q. Zhong, E. Xu, T. Jia, H. Yang, B. Zhang, and Y. Li, "Dynamic performance and control accuracy of a novel proportional valve with a switching technology-controlled pilot stage," *Journal of Zhejiang University-SCIENCE A*, vol. 23, no. 4, pp. 272–285, 2022, https://doi.org/10.1631/jzus.A2100463.

[38] J. Zhang, Z. Lu, B. Xu, and Q. Su, "Investigation on the dynamic characteristics and control accuracy of a novel proportional directional valve with independently controlled pilot stage," *ISA Transactions*, vol. 93, pp. 218–230, 2019, https://doi.org/10.1016/j.isatra.2019.03.023.

[39] H. Zhang, Y. Liao, Z. Tao, Z. Lian, and R. Zhao, "Modeling and Dynamic Characteristics of a Novel High-Pressure and Large-Flow Water Hydraulic Proportional Valve," *Machines*, vol. 10, no. 1, p. 37, 2022, https://doi.org/10.3390/machines10010037.

[40] B. Xu, Q. Su, J. Zhang, and Z. Lu, "Analysis and compensation for the cascade dead-zones in the proportional control valve," *ISA Transactions*, vol. 66, pp. 393–403, 2017, https://doi.org/10.1016/j.isatra.2016.10.012.

[41] Z. Lu *et al*., "Deadzone compensation control based on detection of micro flow rate in pilot stage of proportional directional valve," *ISA Transactions*, vol. 94, pp. 234–245, 2019, https://doi.org/10.1016/j.isatra.2019.03.030.

[42] G. Wrat, M. Bhola, P. Ranjan, S. K. Mishra, and J. Das, "Energy saving and Fuzzy-PID position control of electro-hydraulic system by leakage compensation through proportional flow control valve," *ISA Transactions*, vol. 101, pp. 269–280, 2020, https://doi.org/10.1016/j.isatra.2020.01.003.

[43] P. Dokoupil, D. Himr, and V. Habán, "Experimental analysis of static and dynamic properties of the check valves," *EPJ Web of Conferences*, vol. 213, p. 02013, 2019, https://doi.org/10.1051/epjconf/201921302013.

[44] J. Mi and G. Huang, "Dynamic Prediction of Performance Degradation Characteristics of Direct-Drive Electro-Hydraulic Servo Valves," *Applied Sciences*, vol. 13, no. 12, p. 7231, 2023, https://doi.org/10.3390/app13127231.

[45] F. Xie, R. Zhou, D. Wang, J. Ke, X. Guo, and V. X. Nguyen, "Simulation Study on Static and Dynamic Characteristics of Electromagnet for Electro-Hydraulic Proportional Valve Used in Shock Absorber," *IEEE Access*, vol. 8, pp. 41870–41881, 2020, https://doi.org/10.1109/ACCESS.2020.2976713.

[46] M. Yang, "Study on Dynamic and Static Performance of a Micro Digital Hydraulic Valve," *Micromachines*, vol. 13, no. 5, p. 741, 2022, https://doi.org/10.3390/mi13050741.

[47] G. N. Sahu, S. Singh, A. Singh, and M. Law, "Static and Dynamic Characterization and Control of a High-Performance Electro-Hydraulic Actuator," *Actuators*, vol. 9, no. 2, p. 46, 2020, https://doi.org/10.3390/act9020046.

[48] S. -N. Yun, Y. -L. Lee, H. A. Khan, C. -N. Kang, Y. -B. Ham and J. -H. Park, "Proportional Flow Control Valve for Construction Vehicle," *2019 23rd International Conference on Mechatronics Technology (ICMT)*, pp. 1-3, 2019, https://doi.org/10.1109/ICMECT.2019.8932103.

[49] Y. Gazaz, M. Soliman, M. Abdelrahim, and A. S. A. El-Lail, "Hydraulic Fluid Temperature -Imposed Nonlinearities in Automotive Active Hydraulic Suspension Systems," *JES. Journal of Engineering Sciences*, vol. 52, no. 3, pp. 87-104, 2024, https://doi.org/10.21608/jesaun.2024.226034.1246.

[50] Q. Chen, H. Ji, H. Xing, and H. Zhao, "Experimental study on thermal deformation and clamping force characteristics of hydraulic spool valve," *Engineering Failure Analysis*, vol. 129, p. 105698, 2021, https://doi.org/10.1016/j.engfailanal.2021.105698.

[51] S. Kravets, "Adaptive Influence of Pressure Change of the Hydraulic System of the Hydraulic Drive," *Engineering, Energy, Transport AIC*, vol. 4, no. 119, pp. 55–60, 2022, https://doi.org/10.37128/2520-6168-2022-4-7.

[52] Y. Zhu, Q. Zhang, J. Tao, D. Tan, and X. Wang, "Heat Characteristics Analysis of Electro-Hydraulic Servo Valve," *Journal of Thermal Science and Engineering Applications*, vol. 11, no. 3, p. 031008, 2019, https://doi.org/10.1115/1.4041880.

[53] J. He *et al*., "Experiment and simulation study on cavitation flow in pressure relief valve at different hydraulic oil temperatures," *Flow Measurement and Instrumentation*, vol. 89, p. 102289, 2023, https://doi.org/10.1016/j.flowmeasinst.2022.102289.

[54] B. Wang, X. Zhao, L. Quan, Y. Li, Y. Hao, and L. Ge, "A method for improving flow control valve performance based on active differential pressure regulation," *Measurement*, vol. 219, p. 113271, 2023, https://doi.org/10.1016/j.measurement.2023.113271.